PERGAMON

International Journal of Multiphase Flow 26 (2000) 1851–1873

International Journal of Multiphase Flow

www.elsevier.com/locate/ijmulflow

An improved void fraction model for two-phase cross-flow in horizontal tube bundles

P.A. Feenstra*, D.S. Weaver, R.L. Judd

Department of Mechanical Engineering, McMaster University, Hamilton, Ontario L8S 4L7, Canada

Received 23 June 1999; received in revised form 24 November 1999

Abstract

A physically based model has been developed to predict the void fraction for upward cross-flow through horizontal tube bundles. It agrees well with experimental void fraction measurements in refrigerant 11 and air–water mixtures for a sufficiently wide range of pitch mass flux, quality and P/D ratios. It has also shown improved predictive capability for adiabatic air–water and diabatic R-113 cross-flows than the void fraction models developed by other researchers. The analysis performed also shows plausible applicability of the void fraction model to steam-water data. The present void fraction model will allow researchers and designers to obtain better estimates of void fraction in the shell side flow in applications such as kettle reboilers and the U-bend region of nuclear steam generators than with the customarily used homogeneous equilibrium model. This will result in better estimates of average fluid density and average velocity of two-phase upward cross-flow through horizontal tube bundles.

Keywords: Two-phase flow; Heat exchanger tube bundles; Void fraction

1. Introduction

Two-phase vapour–liquid flow exists in many shell and tube heat exchangers such as kettle reboilers and steam generators. The flow in these devices depends upon a balance between the driving hydrostatic head and the frictional and accelerational pressure drops. These components of pressure drop need to be known in order to model the thermo-hydraulic

* Corresponding author.

PII: S0301-9322(99)00118-4

performance of these devices because a complex interaction exists between the heat transfer coefficient and the average flow velocity across the tubes. The void fraction is needed in order to calculate the hydrostatic and accelerational pressure drop of the flow, because it determines important flow parameters such as average fluid density and average flow velocity at a particular location in the bundle. Accurately determining the average density and effective flow velocity of two-phase flows is difficult because it depends upon the velocity ratio, S, which is defined as the ratio of gas to liquid phase velocity, $S = U_G/U_L$. These parameters are also needed for flow-induced vibration analyses for predicting fluid forces and the fluidelastic instability threshold of a tube array subjected to two-phase flows.

Several authors such as Palen and Yang (1983), Fair and Klip (1983) and Payvar (1983) have presented circulation boiling models to predict the thermo-hydraulic performance of shell and tube boilers, but the lack of a suitable void fraction model led them to use correlations that were originally developed for internal pipe flows. Other researchers such as Whalley and Butterworth (1983) and Leong and Cornwell (1979) used the homogeneous equilibrium model (HEM) to predict void fraction, but this model neglects the effect of the velocity ratio altogether. The applicability of these models to shell-side cross-flow in a tube bundle seems difficult to justify, and with the availability of new data, the pursuit of an improved two-phase void fraction model is warranted.

In recent years, a few articles have been published on the prediction of void fraction in vertical upward flow through tube bundles. Kondo and Nakajima (1980) made indirect void fraction measurements in vertical cross-flow in a bundle but their experiments were performed at very low flow rates ($G_p < 5$ kg/m^{2}s). Schrage et al. (1988) made void fraction measurements in an in-line bundle with air–water cross-flow using quick-closing plate valves. They found that void fraction varied with mass flux and was greatly over-predicted by the HEM model. Therefore, they developed an empirical void fraction model but did not test it against other data. More recently, Dowlati (1992), Dowlati et al. (1990) and Dowlati et al. (1992) measured void fraction using a gamma densitometer in air–water cross-flow experiments in horizontal tube bundles of normal square and normal triangular patterns with pitch-over-diameter (P/D) ratios of 1.3 and 1.75. They found that the HEM significantly over-predicted the void fraction when compared with their gamma densitometer measurements. They developed a model to predict void fraction that was based upon the dimensionless superficial gas velocity, j_G^*, which they argued was an appropriate scaling parameter for vertical upward two-phase flows. Their model agreed well with their own void fraction measurements but was not thoroughly tested due to lack of other appropriate data.

A proper model for predicting void fraction should be applicable to almost any fluid, and preferably should not depend upon a fitting of coefficients specific to only one fluid. Since the literature has recently expanded to include compilation of data for more than one fluid, an attempt has been made to develop a model which is physically based and would give predictions about almost any fluid and would not require the fitting of coefficients for different fluids. This paper presents this new void fraction model for upward two phase cross-flow in horizontal tube arrays. The functional form of the model is physically based and is given specific form using the present authors' measurements in R-11 flow. The model is then used to compute void fraction as a function of quality and mass flux for comparison with other data in the literature.

2. Void fraction model development

2.1. Assessment of previous void fraction models

The development of the present void fraction model arose from the need to compare the present authors' flow-induced vibration data in R-11 cross-flows to other researcher's data, most of which were obtained with air–water mixtures that were supposed to simulate the steam–water mixture in the U-bend region of a nuclear steam generator. Most of the previous researchers did not employ any means of measuring void fraction, and hence they relied on the HEM to determine average fluid density and flow velocity of the two phase cross-flow. However, a proper determination of these quantities requires an appropriate, generally applicable two-phase void fraction model to account for the velocity ratio of the phases. Then a more accurate comparison of the various data sets can be made to determine the threshold flow velocities for fluidelastic instability of tube arrays in cross-flow. Fig. 1 displays the present author's void fraction measurements in R-11 flow along with various void fraction models for three separate mass flux values. The plotted data points (ie., □, △, ○), which were obtained from void fraction measurements using a gamma densitometer, correspond to three different series of experiments, the details of which are explained in Appendix A. The various lines in Fig. 1 are the predictions of Schrage et al. (1988), the void fraction model developed for air–water by Dowlati et al. (1992), the well known Drift Flux model and the HEM. The details of the other void fraction models are summarized in Appendix B. The HEM is an inaccurate predictor since it assumes a velocity ratio of unity. Consequently, the HEM represents a logical upper bound, and no data should plot above this curve because this would imply that the liquid phase was flowing faster than the gas phase. Though the void fraction model of Dowlati et al. (1992) appears reasonable at low mass flux, it was rejected because it violates this criteria at higher mass flux. The drift flux model was also rejected because it did not accurately agree with the R-11 data. Schrage's model appears to be superior to the others for the R-11 data, but this empirical model was considered inadequate because it compared poorly with air–water data of other researchers. Hence there was a need to develop a physically based model for predicting void fraction in two-phase cross-flows in tube arrays which would be applicable to any fluid and would require input parameters that were easily obtainable.

2.2. Theoretical development of the void fraction model

The model development began with the relationship between void fraction, ϵ, and flow quality, x, given by Eq. (1), which is derived from a linear combination of the continuity equation for each phase.

$$\text{Void fraction:} \quad \epsilon = \left(1 + S\frac{\rho_G}{\rho_L}\left(\frac{1}{x} - 1\right)\right)^{-1} \tag{1}$$

Velocity ratio, S, is the ratio of gas velocity to liquid velocity (U_G/U_L) and is the primary unknown in Eq. (1) since quality, x, and gas and liquid phase densities, ρ_G, ρ_L, are usually easy to determine. It was thought prudent to pursue a model to determine velocity ratio rather

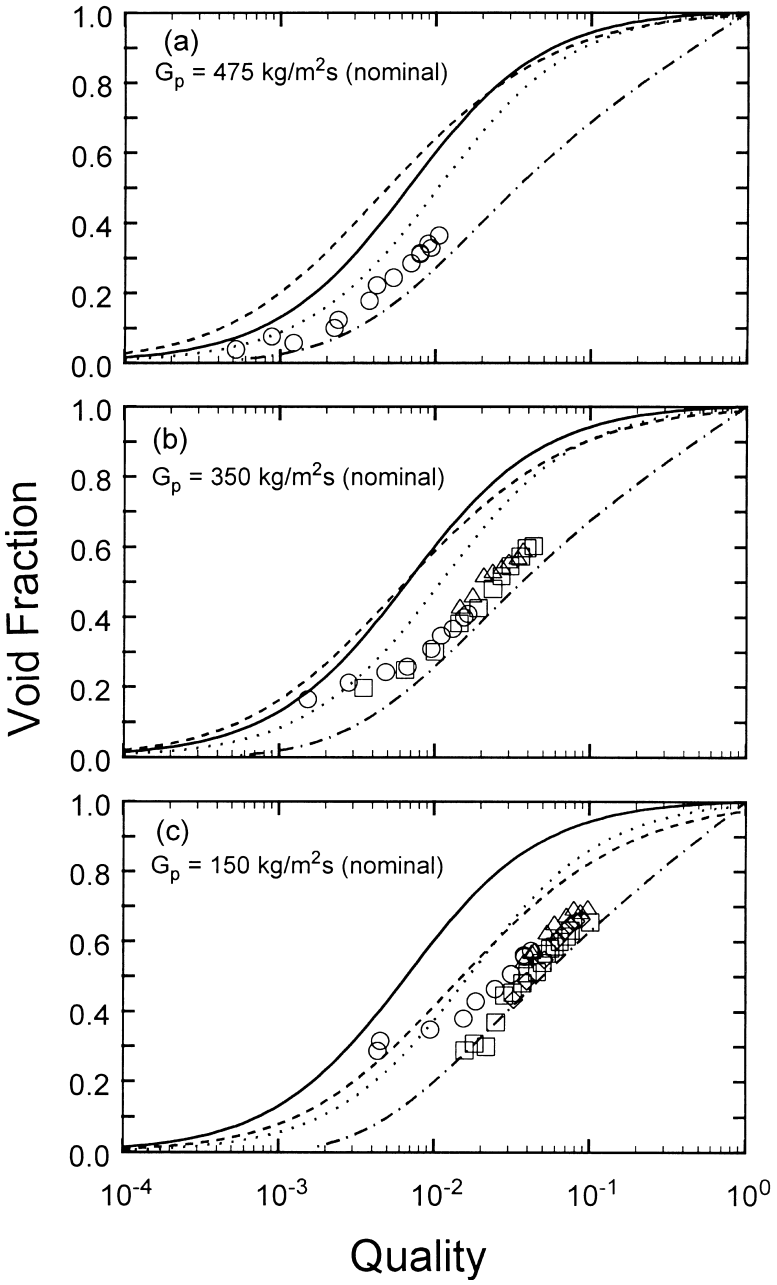

Fig. 1. Void fraction vs. quality for present authors' R-11 data, $P/D = 1.44$. Comparison with existing void fraction models: ——— HEM; - - - - Dowlati et al. (1992); · · · · Drift flux; -·-·- Schrage et al. (1988). Experimental Data: ○ M series; □, ◇ B series; △ C series.

than void fraction (as in Schrage's model) or gas velocity (as in the drift flux model) because then Eq. (1) would automatically obey the boundary conditions at 0% and 100% quality.

The problem was to identify the important variables that affected velocity ratio and to form dimensionless groups that were appropriate to the development of the model. It was clear that the buoyancy of the gas phase was the driving force behind the velocity ratio, without which it would be close to unity. Hence, density difference, $\Delta\rho$, and average two-phase density, ρ, are considered to be key parameters. The viscosity of the liquid phase, η_L, was selected since it affects the ability of the gas bubbles to rise through the liquid. Surface tension, σ, was selected since it affects bubble size and shape. Previous experience showed that the gas phase velocity increased as the bubble size increased, owing to the increased buoyancy of a larger gas bubble. The gap between the tubes, a, was chosen as the characteristic dimension since this is the space through which the flow must pass. Note that this is contrary to some other models which use tube diameter as the characteristic length dimension. The tube diameter, D, and pitch, P, were thought to play a role in velocity ratio, since they influence the frictional pressure drop through the array. The air–water data of Dowlati (1992) and Noghrehkar (1996) has shown that velocity ratio is generally greater for in-line arrays (i.e., normal square) than for staggered arrays (i.e., normal triangular). This indicates that the array geometry also affects the velocity ratio in cross-flow, which is probably the result of the different frictional pressure drops, Δp, among these array types. Eq. (2) expresses the functional dependency of velocity ratio on the previously mentioned variables.

$$S = \frac{U_G}{U_L} = f\left[\Delta\rho, \rho, V_p, \eta_L, \sigma, g, a, P, D, \Delta p\right]. \tag{2}$$

The pitch flow velocity, V_p, is introduced here although it is understood that in two-phase flow it does not have precise meaning unless a fluid model is assumed. However, it is retained here for clearly expressing the dimensionless numbers that follow, while in the final form of the model it is eliminated in favour of other more appropriate quantities. Application of the Buckingham pi theorem permitted reducing the number of variables in Eq. (2) into a smaller number of dimensionless groups which is equal to the number of parameters minus the number of fundamental variables: mass, length and time. Thus, using the gap, a, as the basic length scale,

$$S = f\left[\left(\frac{ga}{V_p^2}\right)^a, \left(\frac{\rho V_p^2 a}{\sigma}\right)^b, \left(\frac{V_p a}{\rho\eta_L}\right)^c, \left(\frac{\Delta p}{\rho V_p^2}\right)^d, \left(\frac{\Delta\rho}{\rho}\right)^e, \left(\frac{P}{a}\right)^f, \left(\frac{D}{a}\right)^g\right] \tag{3}$$

The first four dimensionless groups are the Froude, *Fr*, Weber, *We*, Reynolds, *Re*, and Euler, *Eu*, Numbers. The number of variables can be further reduced by combining two or more groups to form a new variable, which is also dimensionless. This also eliminates some of the repetition in the force scale ratios, since for example the Reynolds number and the Weber number both involve an inertial force scale. The ratio of these two numbers results in the Capillary number,

$$\text{Capillary no.} = \frac{We}{Re} = \frac{\eta_L V_p}{\sigma} \qquad \left(\frac{\text{viscous force}}{\text{surface tension force}}\right). \tag{4}$$

Combining Froude number with density ratio results in the Richardson number,

$$\text{Richardson no.} = \frac{\Delta\rho g a}{\rho V_p^2} \qquad \left(\frac{\text{bouyancy force}}{\text{inertial force}}\right). \tag{5}$$

The length scale ratios P/a and D/a can be combined to eliminate a to give P/D, the so-called pitch ratio, which is commonly used to define tube array geometry. Using these combined forms of the dimensionless groups gives,

$$S = f\left[\left(\frac{\Delta\rho g a}{\rho V_p^2}\right)^a, \left(\frac{\eta_L V_p}{\sigma}\right)^b, \left(\frac{\Delta p}{\rho V_p^2}\right)^c, (P/D)^d\right] \tag{6}$$

Having established possible forms of the relevant dimensionless parameters, the problem became one of determining the precise relationship for velocity ratio and the exponents on the individual dimensionless groups. However, the appropriate representation of parameters such as pitch velocity, V_p, and density, ρ, were not known. Should they represent the individual liquid or gas phase values (i.e., ρ_L or ρ_G) or perhaps the average value interpolated with void fraction (i.e., $\rho = \epsilon\rho_G + (1-\epsilon)\rho_L$)? The appropriate representations were subsequently determined by trial and error, as various forms of Eq. (6) were compared with the void fraction data from the present authors' experiments in R-11 (Feenstra et al., 1995) and more recent unpublished data in R-11.

After testing many correlations, the following form proved to fit the R-11 data well,

$$\text{Velocity ratio} \quad (U_G/U_L): \quad S = 1 + 25.7(Ri * Cap)^{0.5}(P/D)^{-1} \tag{7}$$

In this model, the Richardson number, Ri, has the following form,

$$Ri = \Delta\rho^2 g a / G_p^2. \tag{8}$$

Note that this form differs slightly from the more general form given by Eq. (5) in that the pitch velocity, V_p, has been replaced by the pitch mass flux divided by the average fluid density, G_p/ρ. With this substitution, the numerator would have contained a product of average density times phase density difference, $\rho\Delta\rho$, ($\Delta\rho = \rho_L - \rho_G$) but this has been replaced with density difference squared, $\Delta\rho^2$, which agrees better with the data. This is equivalent to combining the Froude number, ga/V_p^2, with the ratio of phase density difference to average density, squared, $(\Delta\rho/\rho)^2$. The capillary number, Cap, in Eq. (7) has the following form,

$$Cap = \eta_L U_G/\sigma. \tag{9}$$

The capillary number requires knowledge of the surface tension, σ, and of absolute viscosity of the liquid phase, η_L, both of which are readily determined from fluid property tables. To obtain better agreement with the experimental data, the gas phase velocity, U_G, has been used instead of the pitch velocity, V_p, and is determined as follows,

$$U_G = \frac{xG_p}{\epsilon \rho_G} \tag{10}$$

Eq. (10) can be derived from continuity of the gas and liquid phases, assuming both phases are moving in the same direction. The gas phase velocity, U_G, requires a known value of void fraction, ϵ, which depends upon the velocity ratio. Hence, calculating the capillary number is an iterative process whereby the velocity ratio is calculated starting from an assumed value and iterated until the assumed and calculated values agree within a desired degree of precision, which in this case is about 0.5%.

Though the Euler number was proposed in the functional relationship given by Eqs. (3) and (6), it is noticeably absent from the model given by Eq. (7) because, presently, there is insufficient frictional pressure drop data pertaining to the various bundle geometries in various two-phase fluids to determine precisely how it affects the velocity ratio. The frictional pressure drop data obtained by Dowlati (1992) showed unusual trends with respect to array geometry and P/D ratios, which they were unable to explain. Hence it was thought best to exclude The Euler number from the proposed model until further data could reveal clearer trends.

Before concluding this section, mention should be made of the flow regime since it is usually an important factor in any two-phase flow study. Most flow regime analyses have focused on internal pipe flow for vertical and horizontal orientations. There have only been a few studies concerned with shell side cross flow in tube arrays, notably by Grant and Chisholm (1979), by Ulbrich and Mewes (1994) by Noghrehkar (1996). Ulbrich and Mewes proposed a new flow regime map, which they claimed had an 85% rate of agreement with existing data. This was much better than any previous map for shell-side flows through tube arrays. Through analysis of their experimental data and those of various other researchers, they found that only three significant flow regimes existed in shell side flow, namely bubbly, intermittent and dispersed flow, while classical slug flow was not generally observed. Noghrehkar found that, by using a specially designed electrical resistivity probe, the void fractions existing inside the bundle are not necessarily the same as that observed from outside the bundle. In the present analysis, it was thought that a flow regime transition from bubbly to intermittent flow might be a factor affecting velocity ratio, and therefore it would require consideration in the model. Most of the void fraction data examined in this paper corresponds to the bubbly flow regimes while the remainder corresponds to the intermittent flow regime. It appears that the effect of flow regime on velocity ratio in tube bundles is not significant. However, there are still insufficient flow regime data, especially in intermittent and dispersed flow, to allow one to make any general conclusions regarding its effect on velocity ratio.

3. Comparison of void fraction model to R-11 data

Fig. 2 demonstrates the comparison of the new void fraction model with the present authors measurements in R-11 cross-flow. This figure is the same as Fig. 1 except that the models of other researchers are omitted, but the HEM is retained because it represents a logical upper bound to the data. Most of the data points correspond to bubbly flow except for a few at the highest levels of quality indicated in Fig. 2(c), where the onset of intermittent flow was

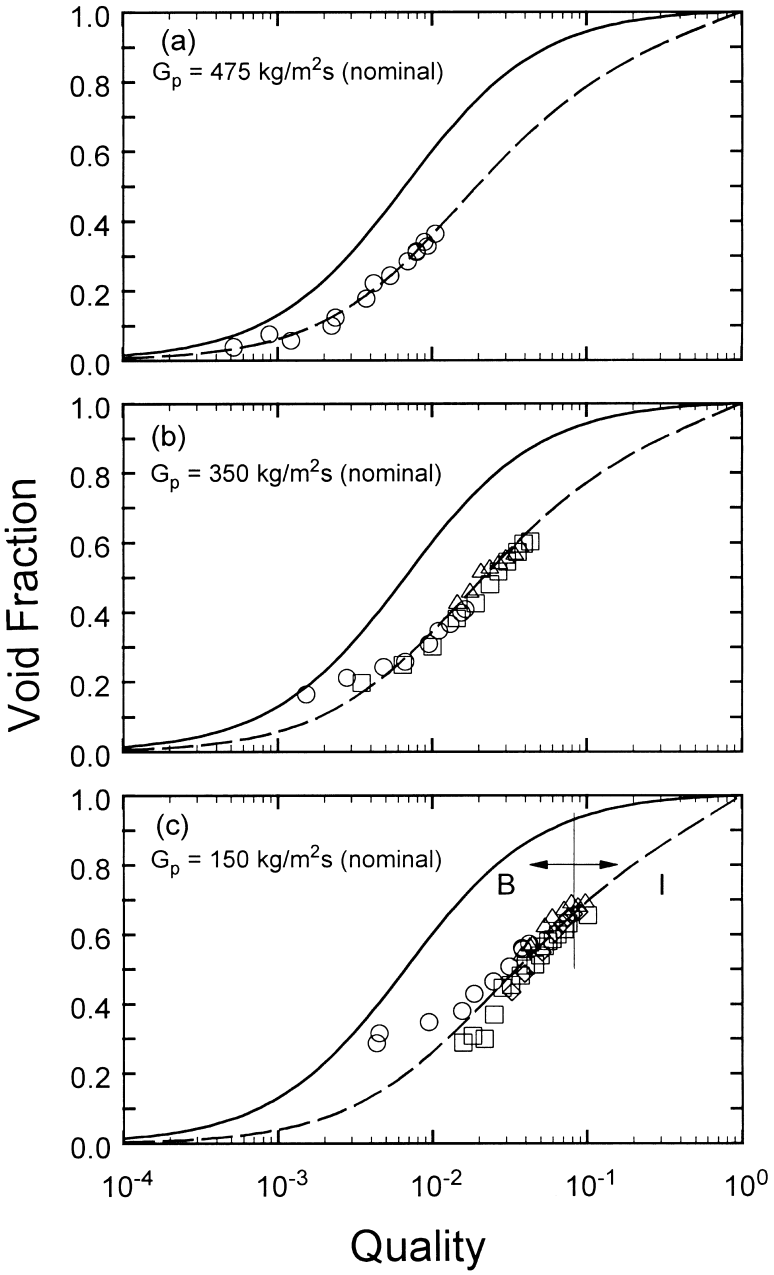

Fig. 2. Void fraction vs. quality for R-11 data, $P/D = 1.44$. Comparison with proposed void fraction model: - - - proposed void fraction model; ——— HEM. Experimental Data: ○ M series; □, ◇ B series; △ C series. Vertical line indicates a flow regime transition from Bubbly to Intermittent flow.

observed. The lack of measurements in the intermittent flow and dispersed flows for the R-11 data makes it impossible to assess any effects of flow regime on velocity ratio.

Clearly, the agreement between the new model and the R-11 void fraction data is very good. Some deviation is noted with certain data points, specifically the 'M' series data indicated by the circles, at the lower qualities, which may be attributable to two factors. One factor is that these measurements were obtained prior to the flow-loop overhaul, in which an upstream turbulence generator was installed to provide better upstream flow conditioning and improvements were made to the vapour condenser to minimize subcooling of the liquid during heat removal. The other factor is that an unavoidably large uncertainty exists in the quality measured at low values as discussed in Appendix A.

4. Comparison of void fraction model with other data

Figs. 3 and 4 show graphs of void fraction vs. quality for three different pitch mass fluxes for the air–water cross-flow data of Dowlati (1992) for $P/D = 1.3$ and 1.75 respectively, obtained at atmospheric pressure conditions. It is clear that the new model follows the trends of the measured void fraction with respect to quality and pitch mass flux as well as or better than Dowlati's model and much better than the other three models. Of course, since this data was the basis for Dowlati's empirical model, it is expected that their model should fit the data reasonably well. Schrage's model is clearly a poor fit to the data, which is puzzling because that model was developed under conditions very similar to Dowlati's data of Fig. 3. The Drift flux model generally over-predicts the void fraction data of Figs. 3 and 4 and overall it is inferior to the new void fraction model.

These figures reveal that the data corresponding to the normal triangular array show a higher void fraction than those of the square array. This may be the result of greater pressure drop in the triangular array geometry, where the flow must follow a more arduous path than in the square array. The latter has straight flow lanes between tubes rows. At present, the new model does not account for this difference in behaviour but, as discussed previously, an additional model parameter which accounts for pressure drop, such as the Euler number, could be developed in future as more data becomes available.

It should be noted that Dowlati et al. (1992) reported a flow regime of dispersed bubbly and churn-turbulent bubbly flow for all their test conditions. According to Ulbrich and Mewes (1994), only three significant flow regimes exist in two-phase vertical cross-flow through a tube bundle: bubbly, intermittent and dispersed, which generally coincides with increasing void fraction. It appears that Dowlati's data fell into the 1st category and that the intermittent and dispersed flow regimes were not encountered. Hence, their data does not lend any insight into the effect of flow regime on velocity ratio.

Fig. 5 presents graphs of void fraction vs. quality for three different pitch mass fluxes for the air–water cross-flow data of Noghrehkar (1996) for $P/D = 1.47$, obtained near atmospheric conditions. The new void fraction model agrees well with this data for the pitch mass flux of 500 kg/m^{2}s shown in Fig. 5(b). For the higher and lower mass fluxes, shown in Fig. 5(a) and (c), the fit is still good but the data appears to be more influenced by mass flux than the previous air–water data (i.e., Figs. 3 and 4). It should be noted however, that these void

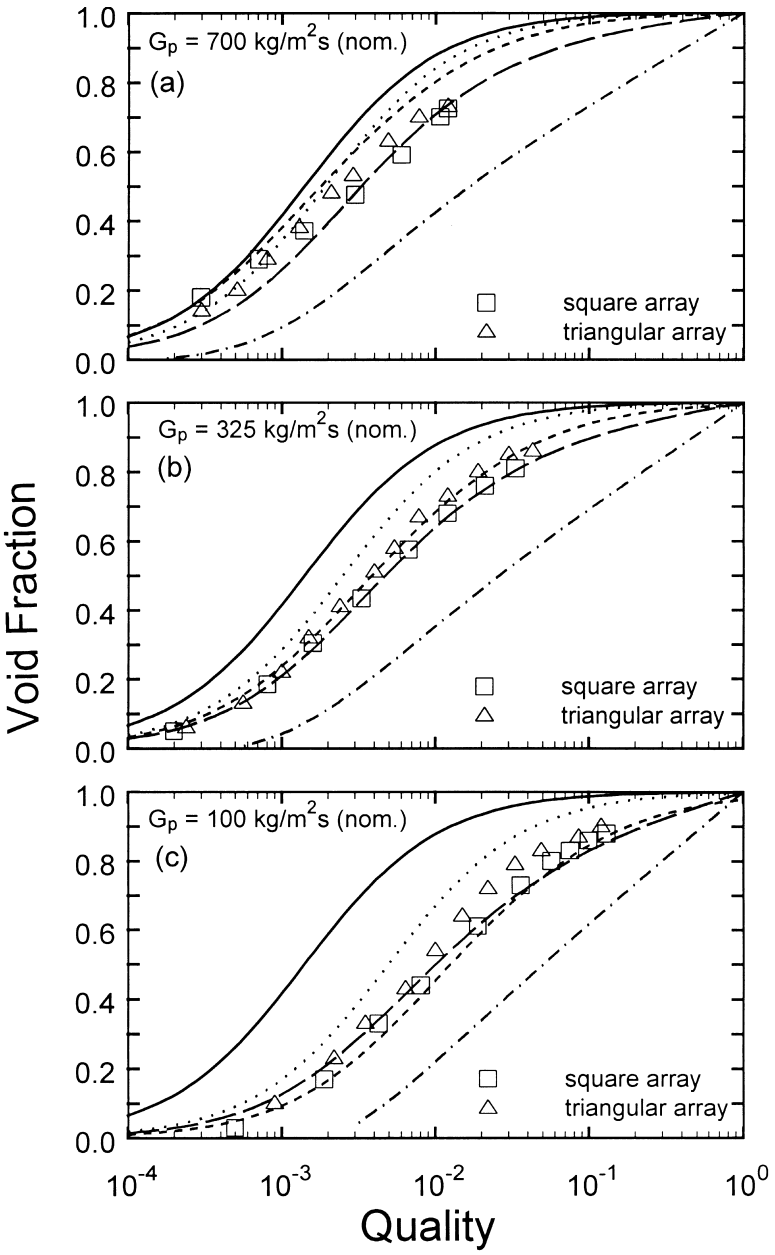

Fig. 3. Void fraction vs. quality for air–water data of Dowlati et al. (1992) $P/D = 1.3$. Comparison with void fraction models: ——— HEM; - - - - Dowlati et al. (1992); · · · · Drift flux; -·-·-· Schrage et al. (1988); — — — proposed void fraction model. Experimental Data: □ square array; △ triangular array.

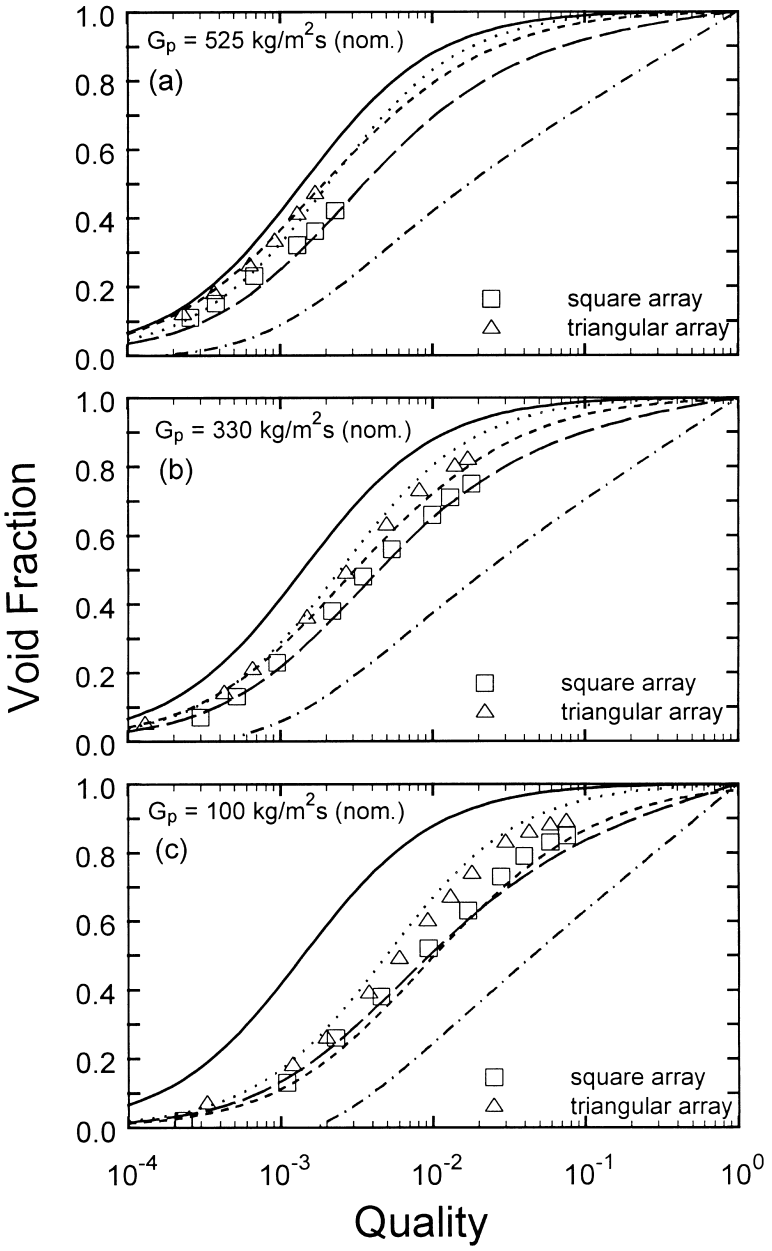

Fig. 4. Void fraction vs. quality for air–water data of Dowlati et al. (1992) $P/D = 1.75$. Comparison with void fraction models: ——— HEM; - - - - Dowlati et al. (1992); · · · · Drift flux, -·-·-· Schrage et al. (1988); — — — proposed void fraction model. Experimental Data: □ square array; △ triangular array.

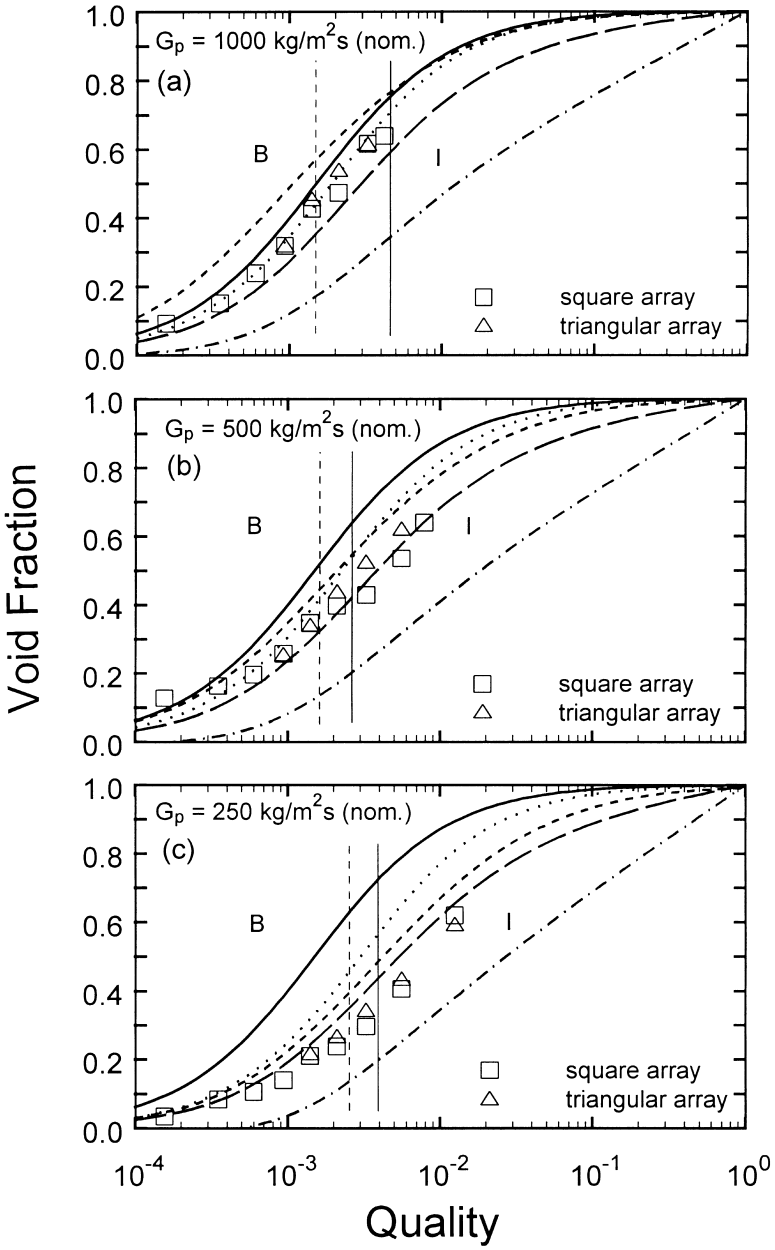

Fig. 5. Void fraction vs. quality for air–water data of Noghrehkar (1996), $P/D = 1.47$. Comparison with void fraction models: ——— HEM; - - - - Dowlati et al. (1992); · · · · Drift flux; ····· Schrage et al. (1988); — — — proposed void fraction model. Experimental Data: □ square array; △ triangular array. Vertical lines indicate transition from Bubbly to Intermittent flow: solid line for triangular array, dashed line for square array.

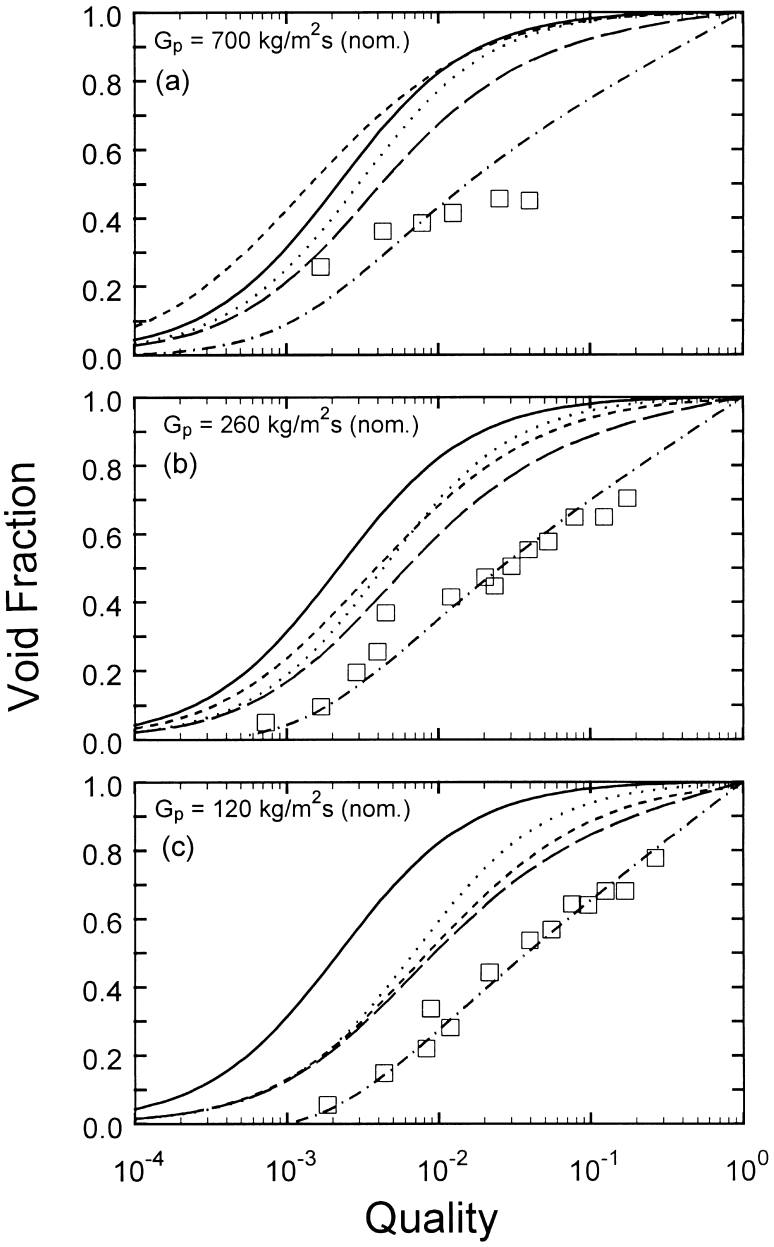

Fig. 6. Void fraction vs. quality for air–water data of Schrage et al. (1988) $P/D = 1.3$. Comparison with void fraction models: ——— HEM; - - - - Dowlati et al. (1992); · · · · Drift flux; ·-·-·-· Schrage et al. (1988); — — — proposed void fraction model.

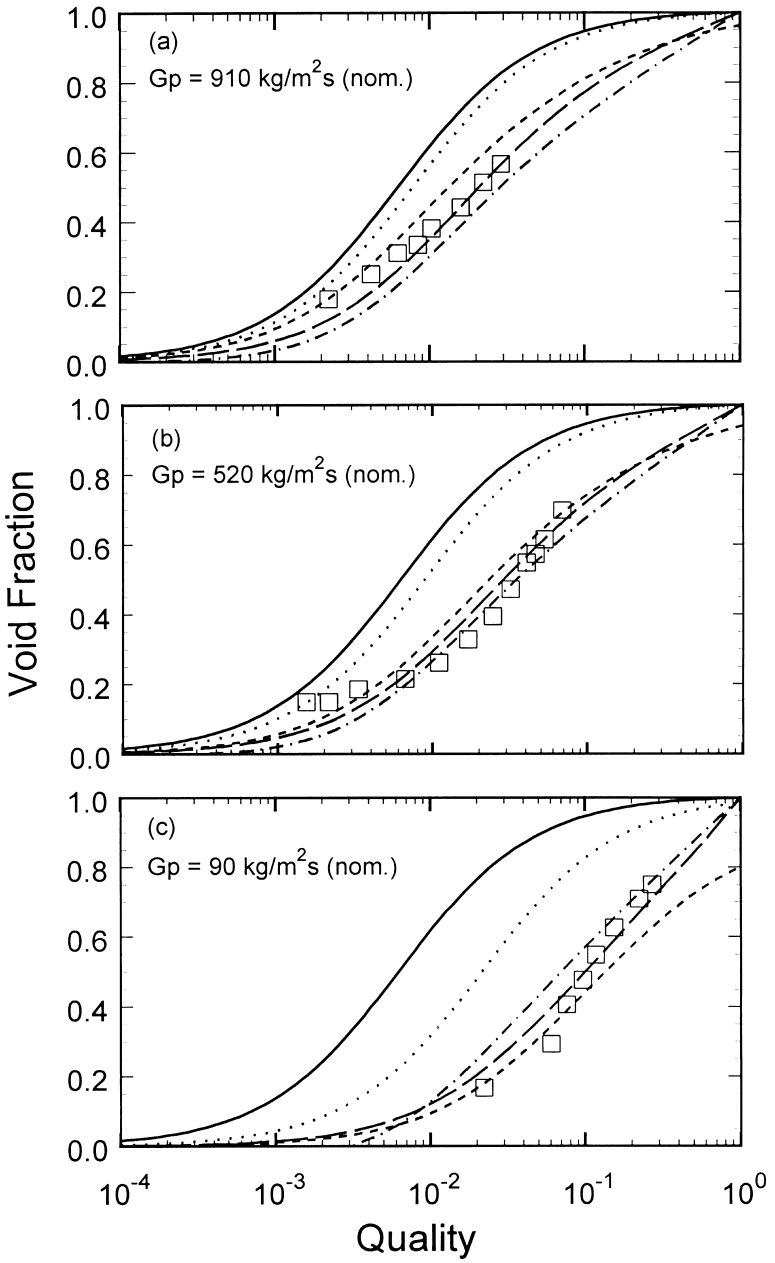

Fig. 7. Void fraction vs. quality for diabatic R-113 data of Dowlati et al. (1996)$P/D = 1.3$. Comparison with void fraction models: ——— HEM; - - - - Dowlati et al. (1996); · · · · Drift flux; ·····Schrage et al. (1988); — — — proposed void fraction model.

fraction measurements were performed in the open area just downstream of the bundle, so exit effects may be a factor. These void fraction measurements also show a slight tendency for lower velocity ratio (higher void fraction) for the triangular array as opposed to the square array.

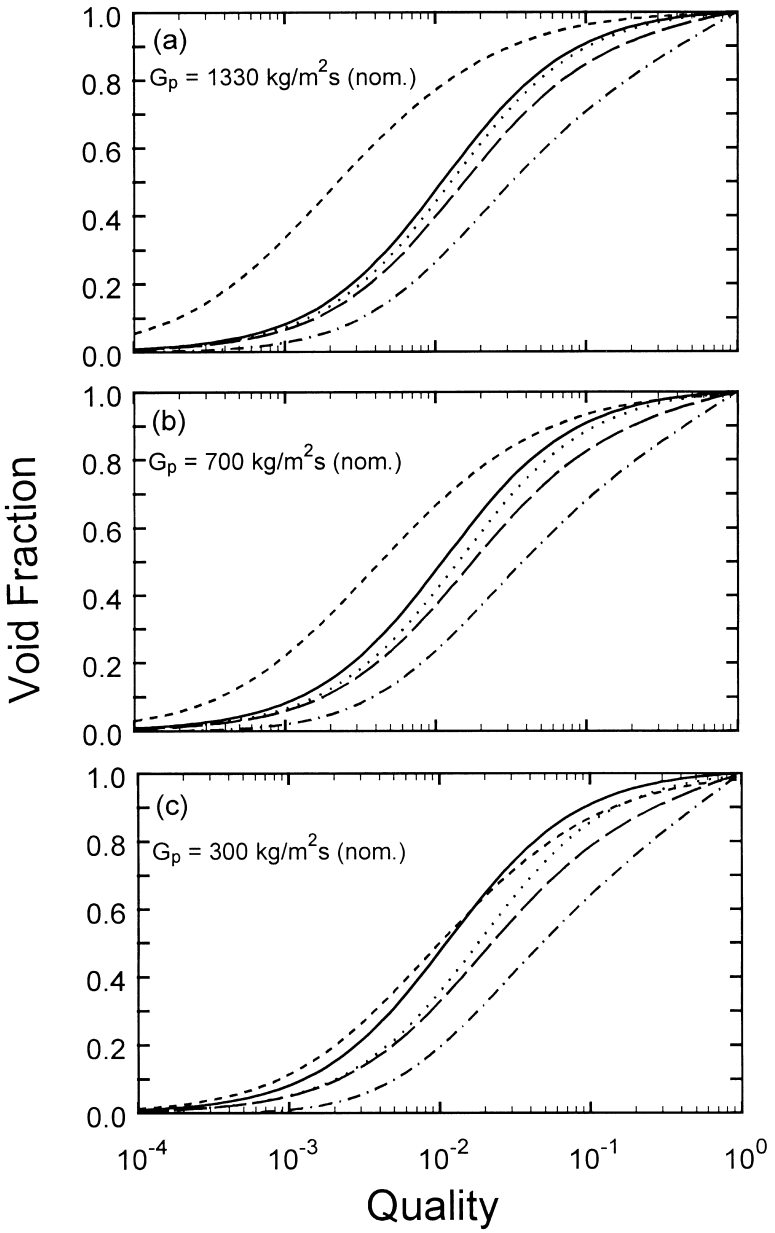

Fig. 8. Void fraction vs. quality for steam–water at conditions tested by Axisa et al. (1985)$P/D = 1.44$. Comparison with void fraction models: ——— HEM; - - - - Dowlati et al. (1992); · · · · Drift flux; -·-·-· Schrage et al. (1988); — — — proposed void fraction model.

Noghrehkar (1996) observed two distinct flow regimes in his experiments, bubbly and intermittent flow, by using a specially designed electrical resistive probe. The transition lines distinguishing the bubbly from the intermittent flows are indicated in Fig. 5(a), (b) and (c) as vertical lines, dashed for the square arrays and solid for the triangular arrays. An important observation to be made in these figures is that Noghrehkar's data shows an insignificant effect of flow regime on the velocity ratio, at least for the bubbly and intermittent flows, which suggests that the new model need not account for these two flow regimes.

Fig. 6 shows the comparison of the present model with the cross-flow data of Schrage et al. (1988)which was obtained in an air–water mixture at atmospheric conditions using quick closing plate valves. The comparison of the present void fraction model does not agree so well with this set of experimental results as in the previous results, and there appears to be no obvious reason for the discrepancy. However, there is a large difference between the void fraction measurements in Schrage's study and those of Dowlati in Fig. 3, to which the present model agrees quite well. The discrepancy between these two researcher's data is puzzling because their experiments were very similar in nature, where the only obvious differences were the void fraction measurement method, the physical size of the test section and tube diameter (see Table 1 for a comparison). It is not clear how these differences could cause the void fraction results to differ so much between these two studies. Since Schrage's data shows some peculiar trends especially at high mass fluxes, it seems reasonable not to put too much significance to its lack of fit with the present model.

It should be noted that, initially, the present model was developed to correspond to the available void fraction data, most of which corresponds to adiabatic flow. Experiments in diabatic flow, with boiling or simulated void fraction generation on the tubes, are scarce (Gidi et al., 1997; Schrage et al., 1988; Hsu, 1987; Dowlati et al., 1996), and the results are difficult to interpret due to the constantly changing flow quality in the tube bundle. A comparison of the boiling flow data of Dowlati et al. (1996) with the void fraction models is shown in Fig. 7. These researchers measured the void fraction of a vertical cross flow of R-113 in a heated, in-line tube array with $P/D = 1.3$. The array consisted of 5 streamwise rows by 20 transverse rows of tubes with 12.7 mm outer diameter. R-113 was boiled on the tube surfaces by means of heated oil which was pumped through all of the tubes. These authors noted that, similar to their adiabatic air–water experiments, mass flux and flow quality had a strong influence on void fraction. The design of their apparatus did not allow visual observation of the flow regime however. The comparison in Fig. 7 shows good agreement between the present model and the R-113 data over a wide range of pitch mass flux. In this case both Schrage's model and Dowlati's model agree reasonably well with the data. It is expected that Dowlati's model should fit the data well since the coefficients used in his model were selected from their paper, which was fitted to that data (ie., $C_1 = 10$ and $C_2 = 1$). It should be re-stated however, that a proper, physically based void fraction model should be applicable to any fluid and preferably should not depend upon a fitting of coefficients that are specific to only one fluid.

In Fig. 8, the predictions of the present void fraction model and the other models are compared for the case of steam–water cross-flow at conditions tested by Axisa et al. (1985) in their flow-induced vibrations experiments. While there were no void fraction measurements obtained in that study, the comparison demonstrates that the void fraction predictions of the

Table 1
Summary of experimental conditions and tube array data

Name	Array type[a]	P/D	Tube diameter (mm)	Array Size	Fluid(s), temperature[b]	Gas phase density, ρ_G (kg/m^3)	Liquid phase density, ρ_L (kg/m^3)
Present Study	PT	1.44	6.35	4×7	R-11, 40°C	9.65	1440
Dowlati et al. (1992)	NS, NT	1.3	19.05	5×20	Air–water, 25°C	1.4	997
Dowlati et al. (1992)	NS,NT	1.75	12.7	5×20	Air–water, 25°C	1.4	997
Noghrehkar (1996)	NS, NT	1.47	12.7	5×24	Air–water, 22°C	1.5	997
Schrage et al. (1988)	NS	1.3	7.94	4×27	Air–water, 10°C	2.2	1000
Dowlati et al. (1996)	NS	1.3	12.7	5×20	R-113, 55°C	9.36	1489
Axisa et al. (1985)	PT	1.44	19.0	11×11	Steam–water, 260°C	23.7	784

[a] PT = Parallel triangular, NS = Normal square (in-line), NT = Normal triangular.
[b] Fluid temperatures are estimated for the air-water studies, all of which were performed near atmospheric conditions.

new model are plausible because the model plots below the HEM curve and exhibits the expected trend with respect to pitch mass flux.

5. Conclusions

A physically based model has been developed to predict the void fraction for vertical upward cross-flow through horizontal tube bundles. It was demonstrated that it agreed well with experimental void fraction measurements in refrigerant 11 and air–water mixtures for sufficiently wide range of pitch mass flux, quality and P/D ratios. It has also shown better predictive capability for these fluids than the void fraction models developed by other researchers. The analysis performed also showed that the void fraction model agreed with the diabatic cross-flow data of refrigerant 113 and showed a plausible applicability to steam–water cross-flow conditions.

The present model will allow researchers and designers to obtain better estimates of void fraction in shell side vertical cross-flow, in applications such as kettle reboilers and the U-bend region of nuclear steam generators than with the customarily used homogeneous equilibrium model. This will result in better estimates of average fluid density and average flow velocity.

The model does not account for differences in array geometry, even though some results in air–water mixtures show that the velocity ratio is higher (void fraction is lower) in normal square arrays and parallel triangular arrays as opposed to normal triangular arrays. This difference may be due to a greater frictional pressure drop in the latter array type, where the flow path is more arduous. At present, the model does not account for this observed difference in velocity ratio, and predictions are better for flows in square and parallel triangular arrays than for normal triangular arrays. In future, two-phase pressure drop data needs to be obtained to establish clear trends with respect to array geometry, void fraction and fluid type. Then, an additional parameter, such as the Euler number, could be introduced into the model to improve agreement with the various array types.

Appendix A. Experimental procedure for R-11 data

The experimental apparatus is described here briefly, while the interested reader can refer to Feenstra et al. (1995) for a more detailed account. The flow-loop, which was primarily designed for studying flow induced vibration in heat exchanger tube arrays, uses refrigerant 11 (R-11) as the working fluid, the properties of which can be found in the ASHRAE Handbook (1993). A gear pump circulates the fluid with a maximum two-phase flow capacity of about $G_p = 500$ kg/m^{2}s. Vapour generation in the R-11 is accomplished by electric heating elements, having a maximum heating capacity of 19.2 kW. The test section, in which the tube bundle is mounted, is a rectangular flow channel with cross-sectional dimensions, 305 mm × 31.8 mm (12 in. × 1.25 in.). The tube bundle consists of 10 cantilevered tubes in a parallel triangular array. Half tubes are installed on the test section wall to minimize the boundary effects. A illustration of the test section and tube array is provided in Fig. A1.

The experimental data plotted in Fig. 1 is subdivided into the different series of experiments

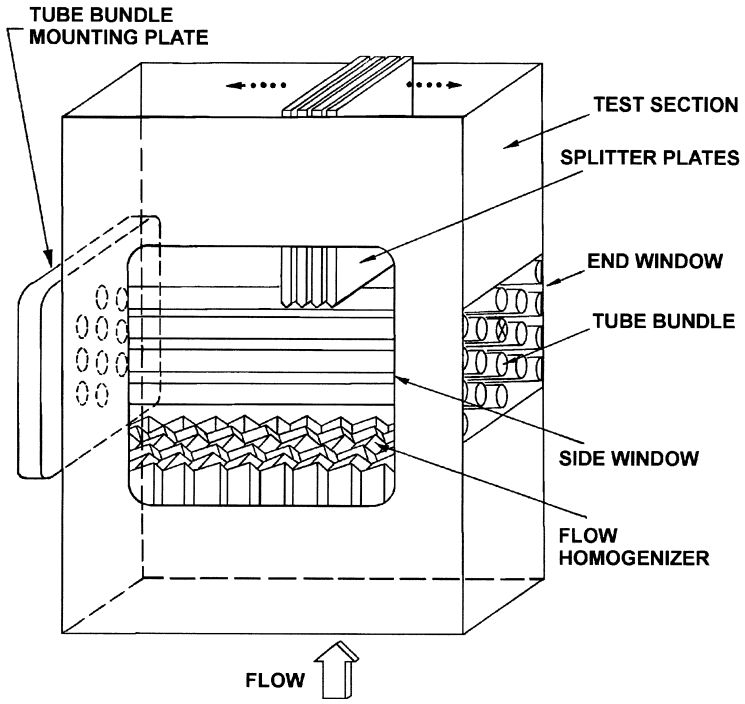

Fig. A1. Sketch of test section and tube bundle used in R-11 flow-induced vibration experiments.

that were performed (ie., M, B, and C series). Series M and B experiments utilized a bundle with tube diameters, $D = 6.35$ mm and a P/D ratio of 1.44, while for the C series of experiments, $D = 6.17$ mm and $P/D = 1.48$. The range of operating pressure varied from one experiment to the other but was typically about 0.17 ± 0.04 MPa (abs.) so that the vapour and liquid densities at the mean pressure were about $\rho_G = 9.7$ kg/m^3 and $\rho_L = 1440$ kg/m^3.

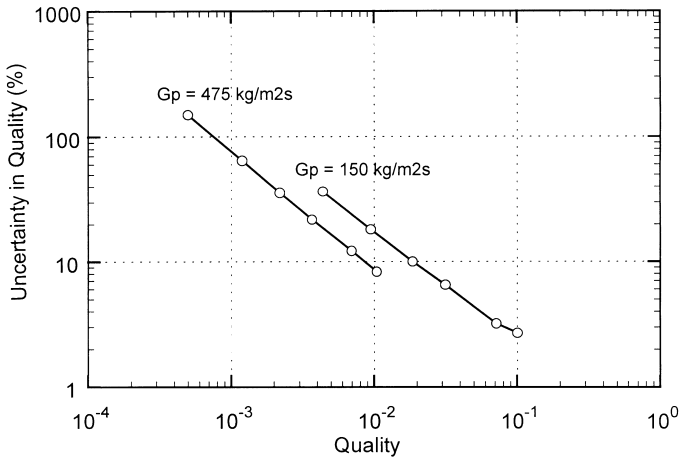

Fig. A2. Uncertainty in quality for R-11 data.

The uncertainty in quality determination is shown in Fig. A2. This was developed based upon the estimated uncertainties in three primary measurements: heater power (±0.05 kW), flow rate (±0.3 l/min) and thermocouple temperature measurement (±0.005 mV). Note that the curves in Fig. A2 represent a worst case combination of these three errors. While the relative error seems excessive at low qualities, it must be remembered that the absolute value of the error is small, and of no great consequence to the accuracy of the model predictions.

Single beam gamma ray attenuation was used to obtain a void fraction measurement of the two-phase R-11 flow in the test section just upstream of the tube bundle. The measurement system consists of a gamma source, lead shielding, a scintillator and the electronics necessary for signal processing. Cobalt 57 was used as a source for the M series of experiments while a Barium 133 source was used in series B and C experiments. The basic principle of this device for measuring void fraction (described in detail in Chan and Banerjee, 1981) is that the gamma flux which penetrates the test section will be attenuated by an amount which depends upon the average density of the two-phase flow. These authors also provide a guideline for estimating the uncertainty in void fraction measurement based upon the error in counting statistics, e_ϵ, as follows,

$$e_\epsilon = \frac{1}{Sn\sqrt{N_\epsilon t}}. \tag{A1}$$

For the Barium 133 source, the sensitivity, Sn, was 39%, the count rate in two phase flow, N_ϵ, was between the count rates of liquid,$N_L = 1260$, and gas, $N_G = 1890$, and the counting period, t, was 20 s. A conservative estimate of uncertainty using Eq. (A1) is about ±1.6%. However, during experiments, the statistical behaviour of the counts was periodically monitored, and the worst case showed a standard deviation of about ±4% of the mean count, N_ϵ, over 5 samples. This leads to a 95% confidence interval ($t_{0.95,\,4} = 2.78$) for void fraction, i.e., a difference of about ±5% of the measurement. This uncertainty is greater than that given by Eq. (A1), and is probably due to flow unsteadiness.

Appendix B. Void fraction models of other researchers

B.1. Void fraction model of Dowlati et al. (1992)

This model was based upon extensive experimental work in vertical air–water void fraction measurements. These authors tested normal square and normal triangular bundles of pitch over diameter ratios of 1.3 and 1.75 each and used gamma densitometry to measure the void fraction in the array, where an average value was obtained from four measurement locations. Their experiments revealed that the homogeneous equilibrium model was insufficient to predict void fraction because it did not account for velocity ratio and the effects of mass flux. It was observed that velocity ratio tended to decrease with mass flux. Since buoyancy was the driving force of the velocity ratio and the mass flux effect was caused by a balance of buoyancy and inertial forces, they used the dimensionless gas velocity, j_G^*, as a controlling parameter,

$$j_G^* = \frac{xG_p}{\sqrt{gD\rho_G(\rho_L - \rho_G)}}. \tag{B1}$$

Subsequently, they found that their void fraction data correlated well using Eq. (B2).

$$\epsilon = 1 - \left(1 + C_1 j_G^* + C_2 j_G^{*2}\right)^{-0.5} \tag{B2}$$

Initially they selected constants $C_1 = 35$ and $C_2 = 1$ respectively as the best fit for square arrays and suggested using $C_2 = 30$ when $j_G^* > 0.2$ (Dowlati et al., 1990). However, in the subsequent paper, (Dowlati et al., 1992), they set constants $C_1 = 30$ and $C_2 = 50$ to give the best overall fit for the square and triangular tube arrays in air–water flow, and these values were used to plot their void fraction model in Figs. 1–6. For R-113 flow, Dowlati et al. (1996) found that $C_1 = 10$ and $C_2 = 1$ provided the best fit, and these values were used to plot their void fraction model in Fig. 7.

B.2. Drift flux model

Zuber and Findlay (1965) proposed a weighted mean velocity of the gas phase, $\bar{U}_G$, given by (B3),

$$\bar{U}_G = C_0(j_G + j_L) + V_B \tag{B3}$$

where $(j_G + j_L)$ is the mixture mean velocity and V_B is the drift velocity which can be interpreted as the rise velocity of bubbles in stagnant liquid. The distribution parameter, C_0, was suggested to be 1.13 by Zuber and Findlay but other researchers have adjusted this constant to better fit their data. For example, Dowlati et al. (1992) used 1.035, while Delenne et al. (1997) used 0.9 which best fit their data for flow across tube bundles. In the present work, $C_0 = 1$ was chosen for comparison with the other models for all the data comparisons so that the boundary condition at $x = 1$ would be satisfied. Following the method of Delenne et al., the drift velocity, V_B, was determined from Eq. (B4),

$$V_B = 1.53\left(\sigma g(\rho_L - \rho_G)/\rho_L^2\right)^{1/4}, \tag{B4}$$

which gives 0.16 m/s for R-11, while for air–water at atmospheric conditions it gives 0.25 m/s which agrees with the experimental measurements of Whalley (1987). For the R-113 data (shown in Fig. 7), the drift velocity was calculated to be $V_B = 0.147$ m/s. The void fraction, ϵ, can be determined as follows,

$$\epsilon = \frac{xG_p}{\rho_G \bar{U}_G}. \tag{B5}$$

B.3. Void fraction model of Schrage et al. (1988)

These authors performed experiments with a normal square bundle subjected to two-phase air–water cross-flow in which the void fraction was measured with quick-closing plate valves

positioned on either end of the bundle. Their measurements revealed that the void fraction was greatly over-predicted by the homogeneous equilibrium model, and was strongly affected by mass flux. A correlation to predict void fraction was developed as shown in Eq. (B6),

$$\epsilon = \epsilon_{\mathrm{H}}\left(1 + 0.123Fr^{-0.191}\ln(x)\right). \tag{B6}$$

Froude number, Fr, was determined by,

$$Fr = G_{\mathrm{p}}/\left(\rho_{\mathrm{L}}\sqrt{gD}\right). \tag{B7}$$

The homogeneous void fraction, ϵ_{H}, was determined by,

$$\epsilon_{\mathrm{H}} = \left(1 + \frac{\rho_{\mathrm{G}}}{\rho_{\mathrm{L}}}\left(\frac{1}{x} - 1\right)\right)^{-1}. \tag{B8}$$

References

ASHRAE Handbook, 1993. Fundamentals, SI Edition, American Society of Heating, Refrigeration, and Air-Conditioning Engineers, Atlanta, GA, pp. 17.1–17.3.

Axisa, F., Boheas, M.A., Villard, B., 1985. Vibration of tube bundles subjected to steam water cross flow: a comparative study of square and triangular arrays. In: Paper B1/2, 8th Int. Conf. on S.M.R.T., Brussels.

Chan, A.M.C., Banerjee, S., 1981. Design aspects of gamma densitometers for void fraction measurements in small scale two-phase flows. Nuclear Instruments and Methods 190, 135–148.

Delenne, B., Gay, N., Campistron, R., Banner, D., 1997. Experimental determination of motion-dependent fluid forces in two-phase water-freon cross flow. In: Païdoussis, M.P., et al. (Eds.), Proceedings of the ASME Int. Symposium on Fluid-Structure Interaction: Aeroelasticity, Flow-Induced Vibration and Noise, AD Vol. 53-2, Vol. II, pp. 349–356.

Dowlati, R., 1992. Hydrodynamics of Two-Phase Cross-Flow and Boiling Heat Transfer in Horizontal Tube Bundles. Ph.D. Thesis, Univ. of Toronto, Dept.of Chemical Engineering and Applied Chemistry, Toronto, Canada.

Dowlati, R., Kawaji, M.D., Chisholm, D., Chan, A.M.C., 1992. Void fraction prediction in two-phase flow across a tube bundle. AIChE J 38, 619–622.

Dowlati, R., Kawaji, M., Chan, A.M.C., 1990. Pitch-to-diameter effect on two-phase flow across an in-line tube bundle. AIChE J 36, 765–772.

Dowlati, R., Kawaji, M., Chan, A.M.C., 1996. Two-phase crossflow and boiling heat transfer in horizontal tube bundles. ASME J. of Heat Transfer 118, 124–131.

Fair, J.R., Klip, A., 1983. Thermal design of horizontal reboilers. Chem. Eng. Prog 79, 86–96.

Feenstra, P.A., Judd, R.L., Weaver, D.S., 1995. Fluidelastic instability in a tube array subjected to two-phase R-11 cross-flow. J. Fluids and Structures 9, 747–771.

Gidi, A., Weaver, D.S., Judd, R.L., 1997. Two-phase flow-induced vibrations of tube bundles with surface boiling. In: Païdoussis, M.P., et al. (Eds.), Proceedings of the ASME Int. Symposium on Fluid-Structure Interaction: Aeroelasticity, Flow-Induced Vibration and Noise, AD Vol. 53-2, Vol. II, pp. 381–389.

Grant, I.D.R., Chisholm, D., 1979. Two-Phase Flow on the Shell Side of a Segmentally Baffled Shell-and Tube Heat Exchanger. ASME Journal of Heat Transfer 101, 38–42.

Hsu, J.T., 1987. A Parametric study of Boiling Heat Transfer in Horizontal Tube Bundles. Ph.D. thesis, University of Wisconsin, Milwaukee.

Kondo, M., Nakajima, K.I., 1980. Experimental investigation of Air–Water two-phase upflow across horizontal tube bundles. Bull. JSME 23, 385–393.

Leong, L.S., Cornwell, K., 1979. Heat transfer coefficients in a reboiler tube bundle. The Chem. Engineer 343, 219–221.

Noghrehkar, G., 1996. Investigation of Local Two-Phase Parameters in Cross Flow-Induced Vibration of Tubes in Tube Bundles. PhD Thesis, Department of Chemical Engineering and Applied Chemistry, University of Toronto, Toronto, Canada.

Palen, J.W., Yang, C.C., 1983. Circulation boiling model for analysis of kettle and internal reboiler performance. In: Kitto, J.B., Robertson, J.M. (Eds.), Heat Exchangers for Two-Phase Applications, HTD-Vol. 27. ASME, New York, pp. 55–61.

Payvar, P., 1983. Analysis of performance of full bundle submerged boilers. In: Two-phase heat exchanger symposium, HTD-Vol. 44. ASME, New York, pp. 11–18.

Schrage, D.S., Hsu, J.T., Jensen, M.K., 1988. Two-phase pressure drop in vertical cross flow across a horizontal tube bundle. AIChE J 34, 107–115.

Ulbrich, R., Mewes, D., 1994. Vertical, upward Gas–Liquid two-phase flow across a tube bundle. Int. J. Multiphase Flow 20, 249–272.

Whalley, P.B., Butterworth, D., 1983. A simple method for calculating the recirculating flow in vertical thermosyphon and kettle reboilers. In: Heat Exchangers for Two-Phase Applications, HTD-Vol. 27. ASME, New York, pp. 47–53.

Whalley, P.B., 1987. Boiling Condensation and Gas–Liquid Flow. Oxford University Press, New York.

Zuber, N., Findlay, J.A., 1965. Average volumetric concentration in two-phase flow systems. ASME J. Heat Trans 87, 453–468.